

# Highly transverse convoy electron distributions emitted by highly charged ions

M. Seliger<sup>a</sup>, K. Tókési<sup>b</sup>, C. O. Reinhold<sup>c</sup>, and J. Burgdörfer<sup>a</sup>

<sup>a</sup>*Inst. for Theoretical Physics, Vienna University of Technology, Austria*

<sup>b</sup>*ATOMKI, Debrecen, Hungary*

<sup>c</sup>*Physics Division, Oak Ridge National Laboratory*

---

## Abstract

We present a theoretical study of convoy electron emission resulting from highly charged ion (HCI) transport through carbon foils. Employing a classical transport theory (CTT) we analyze the angular and energy distribution formed by multiple scattering of electrons in the solid. We find that the convoy electron distribution becomes highly transverse at intermediate foils thicknesses representing an oblate spheroidal distribution due to the stepwise excitation of the HCI. The calculated convoy electron spectra are found to be in good agreement with recent measurements.

*Key words:*

---

---

*Email address:* [marek@concord.itp.tuwien.ac.at](mailto:marek@concord.itp.tuwien.ac.at) (M. Seliger).

*URL:* <http://dollywood.itp.tuwien.ac.at/~marek/> (M. Seliger).

## 1 Introduction

The angular and energy distributions of electrons emitted in ion-atom and ion-solid collisions have been studied extensively (1; 2) during the last few decades, mostly in the regime of non-relativistic projectile velocities. One of the most prominent features of these emission spectra is that in the forward direction they exhibit a cusp-shaped peak at the energy corresponding to the same velocity as the incident ion. Mainly two processes are responsible for this electron emission: the electron loss to the continuum (ELC) originating from a direct transition from the initial state of the projectile electron to the low-lying continuum of the ion (3) and the capture of a target electron to the low-lying continuum of the projectile, electron capture to continuum (ECC)(4). In ion-solid collisions, a similar feature appears in the electron emission spectrum and is commonly referred to as convoy electron peak (CEP) (1). Its origin is far more complex as a multitude of collision processes open alternative pathways to populating these final states. Very recently, measurements of the CEP at relativistic projectile velocities for hydrogenic projectiles have become available (5). As a result of the vanishingly small cross section for ECC at very high velocities, loss from the projectile by stepwise excitation and multiple scattering of liberated electrons can be identified as the main source of the CEP in this case.

Extending our previously developed classical transport theory (CTT) (6; 7) for evolution of hydrogenic projectile states during transmission through solids, we investigate in this communication the convoy electron emission by (moderately) relativistic projectile transmitted through solids. We focus on  $\text{Ar}^{17+}$  ion with an energy of 390 MeV/amu traversing thin self-supporting amorphous

carbon foils of thickness varying from 25 to 9190  $\mu\text{g}/\text{cm}^2$ . This collision system has several attractive features: In the relativistic velocity regime the average distance between two collisions, the mean free path, is long. The thinnest carbon foils available have a thickness of the order of the collisional mean free path, thus providing a testing ground for the limit of single collisions. By varying the foil thickness we have the opportunity to follow the time evolution of the projectile for up to several hundred collisions. In this multiple scattering regime the transient build up of a highly transverse angular distribution in the CEP be can observed. The latter is closely related to ELC from Rydberg states in the gas phase for which we have previously found approximately oblate spheroidal angular distribution under single collision conditions (8). In the present case we find that multiple scattering in the solid leads initially to the build-up of a transient population of Rydberg-like states of the HCl. Ionization of such states in subsequent collisions gives rise to a highly transverse angular distribution. As the collision sequence continues for thick foils, the angular distribution gets distorted due to the slowing down of the convoy electrons in further electron-electron collisions. Comparison with recent experimental data show excellent agreement and confirms this scenario. Atomic units ( $|e| = m_e = \hbar = 1, c = 137$ ) will be used unless otherwise stated.

## 2 Brief outline of the theoretical description

The initial state of the electron is represented within the classical transport theory (CTT) by a probability density in phase space which is initially given by a microcanonical distributions with the binding energy of the projectile electron in the ground state ( $\text{Ar}^{17+}(1s)$ ). The time evolution is given by a

reduced Liouville equation which is solved by test particle discretization, i.e. a Monte Carlo method (6; 7). The dynamics of each test particle is governed by a Langevin equation involving both a deterministic Coulomb force and a stochastic force acting on the electron

$$\dot{\vec{p}} = -\frac{Z_P \vec{r}}{r^3} + \sum_i \Delta \vec{p}_i \delta(t - t_i) , \quad (1)$$

where  $Z_P$  is the projectile charge. Here and in the following  $(\vec{r}, \vec{p})$  denote the position and the momentum of the electron in the projectile frame whereas primed variables as  $(\vec{r}', \vec{p}')$  correspond to the target frame. Outside the solid the time evolution of the electron attached to the projectile is determined only by the central Coulomb force represented by the first term of the Langevin equation (1). In a classical picture the unperturbed electronic motion can be characterized by Kepler orbits with constant energy (9). Inside the solid the interaction with target electrons and nuclei results in a stochastic series of collisions described by a stochastic force (second term in (1)) acting on the electron in addition to the Coulomb force. The very high projectile velocity ( $v_p = 97a.u.$ ) allows us to treat the electron-solid interaction in the impulsive momentum transfer approximation, i.e. momenta  $\Delta \vec{p}_i$  are transferred instantaneously at collision times  $t_i$  reducing the transport problem to a random walk of the projectile electron along Kepler orbits subject to a stochastic sequence of momentum transfers. The probability distribution of  $\Delta \vec{p}_i$  is determined from the relativistic differential inverse mean free path, whereas the flight times  $\Delta t_i$  between two collisions are obtained from the corresponding integral inverse mean free path. The collisions described by  $\Delta \vec{p}_i$  and  $\Delta t_i$  are the scattering of the electron at the screened ionic cores and at target electrons in the solid. Details are discussed elsewhere (7; 10). After the projectile elec-

tron exits the foil, collisional momentum transfers and hence the stochastic force cease to be effective but the long range Coulomb interaction between the electron and the ionized projectile requires continuation of the time evolution to  $t \rightarrow \infty$  in order to determine the asymptotic final state.

### 3 Convoy electron emission

Convoy electron emission is a subset of all ionization events converting  $Ar^{17+}$  into  $Ar^{18+}$ . Fig. 1 displays the evolution of the excited state population (or probability) of  $Ar^{17+}$ . The excited-state evolution shows clear signatures of single- and multi step excitations prior to ionization. Initially, the electron is in the ground state ( $n = 1$ ). Since the energy gap separating it from the nearest higher shell is large ( $\Delta E = 120 a.u.$ ), the required minimum momentum transfer is rather large ( $\Delta p_{min} = 1.3 a.u.$ ) and thus mainly electron-ion core collisions are strong enough to contribute to the excitation process of this state. Because the ground state is depopulated by only one process with a constant probability and the reverse process of increasing its population is very unlikely, the population probability of the ground state obeys an exponential decay law as a function of propagation distance.

The other levels develop a very different behavior. Initially they are populated by transitions from the ground state. In the region of very thin foils this excitation process ( $n = 1 \rightarrow n > 1$ ) is dominant and the relative populations increase very fast by orders of magnitude. Transitions from a certain  $n > 1$  level into higher excited states becomes significant at  $d \gtrsim 2 \times 10^4 a.u. \sim 200 \mu g/cm^2$ . For thicker foils an almost constant ratio between the various n-levels develops.

We investigate now the energy and angular distribution of emitted electrons. Fig. 2 displays the contour lines of the longitudinal  $v'_{\parallel} = (v_{\parallel} + v_p)/(1 + v_{\parallel}v_p/c^2)$  and the transverse ( $v'_{\perp}$ ) velocity distribution of convoy electrons for 9 different propagation distances from the single-collision regime to the multiple scattering regime involving up to hundred of collisions. The velocity vector  $\vec{v}$  refers to the frame of the projectile and prime quantities refer to the lab frame. For the thinnest foil ( $d = 25 \mu\text{g}/\text{cm}^2$ ) the dominant emission process is direct ionization from the ground state (see Fig. 1) resulting in a near-isotropic distribution with a weak enhancement in the transverse direction. For longer propagation distances ( $d \gtrsim 200 \mu\text{g}/\text{cm}^2$ ) the distribution becomes highly transverse reflecting the multi-step ionization of convoy electrons through a sequence of intermediate excited and Rydberg states. Finally, for very thick foils ( $d \gtrsim 3000 \mu\text{g}/\text{cm}^2$ ) the distribution increasingly resembles the Newton circle however shifted toward lower parallel velocities  $v'_{\parallel} < v_p$ . The latter is due to the slowing down of convoy electrons in inelastic electron-electron collisions representing "post-ionization" effects.

The build up of a highly transverse two-dimensional velocity distribution  $P(\vec{v})$  at intermediate distances can be most conveniently parametrized in terms of a multipole expansion of the CEP (11) in the rest frame of the projectile ion,

$$P(\vec{v}) = \frac{d\sigma(v)}{dv} = \frac{\sigma_0(v)}{v} \left( 1 + \sum_{k=1}^{\infty} \beta_k(v) P_k(\cos \theta) \right) \quad (2)$$

where  $P_k(\cos \theta)$  are the Legendre polynomials of the order  $k$  as a function of the polar angle  $\theta$ . The anisotropy coefficients  $\beta_k(v)$  are given by

$$\beta_k(v) = (k + 1/2) \frac{v}{\sigma_0(v)} \int d(\cos \theta) P_k(\cos \theta) \frac{d\sigma(v)}{dv} \quad (3)$$

with  $\sigma_0(v) = v\beta_0(v)$  parameterizing the angle-integrated probability. Fig. 3 shows the multipole expansion for electrons emitted in the transport through a layer of  $2500a.u.$  of carbon ( $d = 25 \mu g/cm^2$ ) while in Fig. 4 we show the average  $\beta_k(v)$  in the significant region for the CEP (up to  $v \leq 1a.u.$ ).

This multipole expansion shows a number of interesting properties:  $\sigma_0(v)$  represents the overall intensity at the given radial velocity  $v$  with the well-known cusp singularity proportional to  $1/v$  factorized out. The first order-term  $P_1(\cos \theta) = \cos \theta$  describes, to leading order, the forward-backward asymmetry in the spectrum. The term  $P_2(\cos \theta)$  represents the intensity distribution of a Hertz dipole associated with dipole transitions. The key point is now that due to multiple scattering as well as "hard" collisions high-order anisotropies are introduced well beyond the dipole limit. With increasing foil thickness, the expansion coefficients of higher-order even multipoles,  $\beta_k(v)$ , increase.

For intermediate propagation distances,  $d < 1000 \mu g/cm^2$ , the distribution is dominated by a large number of *even* multipoles which in both magnitude and sign closely resemble the expansion of spheroidal harmonics,  $S_{mn}(\cos \theta, c)$ , in terms of the Legendre polynomials  $P_k(\cos \theta)$ , with the parameter  $c$  being a measure for the ratio of the focal length to the wave length in the spheroidal wave function (12). As shown by Szabó et al. (8)  $S_{00}(\cos \theta, c)$  describes the differential cross section  $d\sigma/dv$  of a Rydberg electron emitted in a single collision with a gaseous target quite well. This function represents a strongly transverse, oblate spheroidal distribution. In view of the build up of excited states (Fig. 1) our present results are easily understood. With increasing path length, multiple collisions (mostly with ionic cores) sequentially build up transient population of highly excited bound states of the HCl. Subsequent collisions, in turn, result in bound to continuum transitions and hence convoy electron

emission. As the magnitude of average momentum transfer  $|\Delta p_i|$  is, in general, large compared to the characteristic momentum distribution,  $p_n = Z/n$ , for large  $n$ , the resulting angular distribution deviates strongly from the "soft" or dipole limit giving rise to the oblate distribution. It is worth noting that the present calculation of the angular distribution of the CEP is solely based on classical dynamics while the calculation of ELC emission from Rydberg atoms in single collisions was based on a quantum treatment in the first Born approximation (8). It is well known that classical calculations fail to converge to the dipole limit (13) for soft collision  $|\Delta p| \rightarrow 0$ . The fact that  $|\Delta p/p_n| > 1$  is a prerequisite for a strongly oblate spheroidal distribution is also partly responsible for the good agreement between the CTT and the quantum calculation since the relevant ionization process is far from the dipole (or Bethe) limit.

For longer propagation distances, odd multipoles become sizable signaling the shift of the distribution to lower velocities in the lab frame. In general, the multipole parameters  $\beta_k$  depend on  $v$ . Fig. 3 indicates, however that odd multipoles increase linearly with  $v$  while even multipoles approach a finite limit as  $v \rightarrow 0$ .

#### 4 Comparison with experiments

In order to compare our predictions for the present system with recent experimental data (9) we convolute the simulated convoy electron spectra with the experimental angular and energy acceptance of the detector. A small aperture after the foil confines the acceptance angle to  $\Delta\theta = \pm 1^\circ$ . The energy acceptance of the semi-conductor detector is  $\Delta E = \pm 9keV$  centered around the nominal kinetic energy. The three different frames in Fig. 5 pertain to

the three different regimes accessible: Fig. 5(a) displays the convoy peak in the (approximate) single-collision regime with a cusp shape dominated by  $\beta_2$ . Fig. 5(b) is a much narrower CEP reflecting the oblate spheroidal distributions analyzed in the previous section. Finally Fig. 5(c) displays a drastically broadened and shifted CEP that is subject to a large number of slowing collisions subsequent to ionization. For all three cases we find excellent agreement with experimental data confirming, among other properties, the highly anisotropic emission pattern at intermediate propagation distances.

In summary, study of convoy electron emission induced by moderately relativistic HCI's allows the study of the evolution of the CEP from the near single-collision limit to the true multiple scattering regime involving up to hundreds of electron-ion core and electron-electron collisions. The current classical transport theory (CTT) based on a Monte Carlo solution of a microscopic Langevin equation is capable to describe this complex evolution process, including the transient build-up of a high degree of anisotropy, quite well. A more complete comparison between the experiment and theory is in progress (14).

## 5 Acknowledgements

We thank to Y. Yamazaki and his colleagues for providing us with data prior publication. The work was supported by the Austrian FWF. COR acknowledges support by the DCS, OBES, USDOE, managed by UT-Battelle, LLC, under contract DE-AC05-00OR22725.

## References

- [1] M. Breinig, S. B. Elston, S. Huldt, L. Liljeby, C. R. Vane, S. D. Berry, G. A. Glass, M. Schauer, I. A. Sellin, G. D. Alton, S. Datz, S. Overbury, R. Laubert, and M. Suter, *Phys. Rev. A* **25**, 3015 (1982) and refs. there in.
- [2] J. P. Gibbons, S. B. Elston, K. Kimura, R. DeSerio, I. A. Sellin, J. Burgdörfer, J. P. Grandin, A. Cassimi, X. Husson, L. Liljeby, and M. Druetta, *Phys. Rev. Lett.* **67**, 481 (1991).
- [3] J. Burgdörfer, M. Breinig, S. B. Elston, and I. A. Sellin, *Phys. Rev. A* **28**, 3277 (1983).
- [4] M. Lucas, W. Streckelmacher, J. Macek, and J. Potter, *J. Phys. B* **13**, 4833 (1980).
- [5] Y. Takabayashi, T. Ito, T. Azuma, K. Komaki, Y. Yamazaki, H. Tawara, M. Torikoshi, A. Kitagawa, E. Takada, and T. Murakami, *Convoy electron production and ionization in 390 MeV/u Ar<sup>17+</sup> ion collisions with thin foils*. Abstract book of 21<sup>st</sup> ICPEAC, 730 (1999).
- [6] J. Burgdörfer, and J. Gibbons, *Phys. Rev. A* **42**, 1206 (1990).
- [7] B. Gervais, C. O. Reinhold, and J. Burgdörfer, *Phys. Rev. A* **53**, 3189 (1996).
- [8] G. Szabó, J. Wang, and J. Burgdörfer, *Phys. Rev. A* **48**, 3414 (1993).
- [9] H. Goldstein, *Classical mechanics*. (1991) AULA-Verlag Wiesbaden.
- [10] M. Seliger et al., to be published
- [11] W. Meckbach, I. Nemtovski, and C. Garibotti, *Phys. Rev. A* **24**, 1793 (1981).
- [12] J. A. Stratton, P. M. Morse, L. J. Chu, J. D. C. Little, and F. J. Corbató, *Spheroidal Wave Function*, (MIT press and Willey, New York, 1955).
- [13] C. Reinhold and J. Burgdörfer, *J. Phys. B* **26**, 3101 (1993).

- [14] Y. Takabayashi, T. Ito, T. Azuma, K. Komaki, Y. Yamazaki, H. Tawara, E. Takada, T. Murakami, M. Seliger, K. Tórkési, C. O. Reinhold, and J. Burgdörfer, to be published.

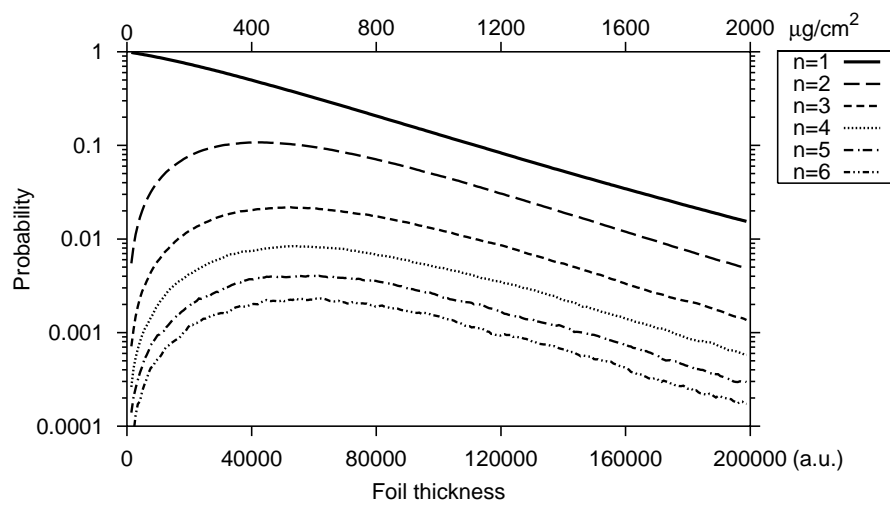


Fig. 1. Probability distribution of the electron initially attached to the projectile ion during the passage through the target in terms of the principal quantum number  $n$  of the atomic states of the  $\text{Ar}^{17+}$  projectile.

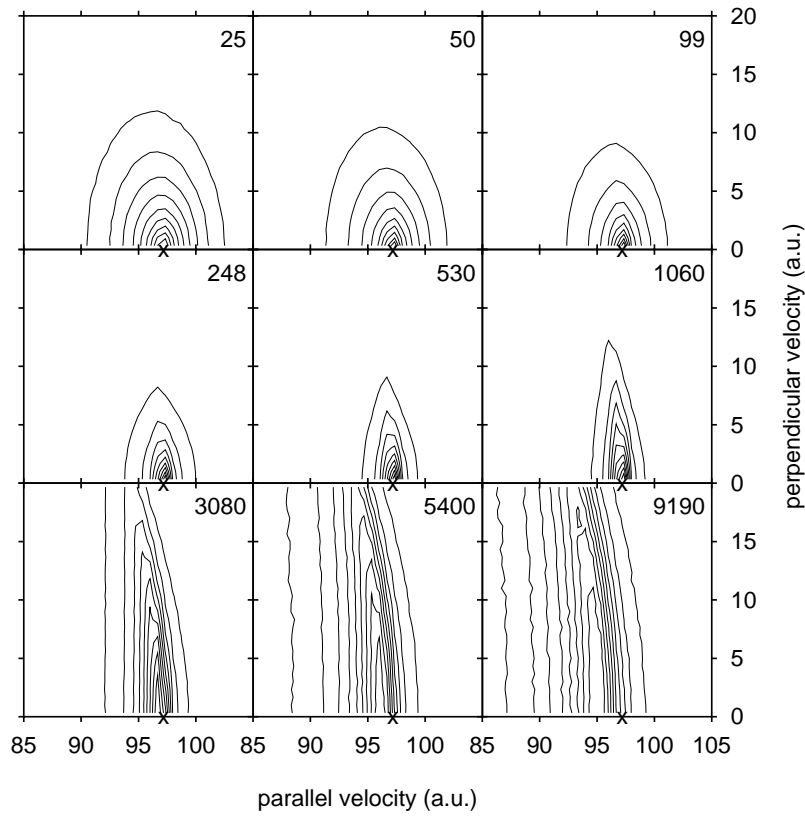


Fig. 2. Contour lines (0.1,0.2,...,0.9) of the velocity distribution (in a.u.) of simulated convoy electrons emitted by an  $\text{Ar}^{17+}$  (390 MeV/amu) in transport through a carbon foil. The foil thickness in units of  $\mu\text{g}/\text{cm}^2$  is denoted for every graph in the top right and the intensities have been normalized to one. The horizontal direction corresponds to the velocity parallel to the projectile ion. The initial projectile ion velocity of  $v = 97 \text{ a.u.}$  is denoted by a cross.

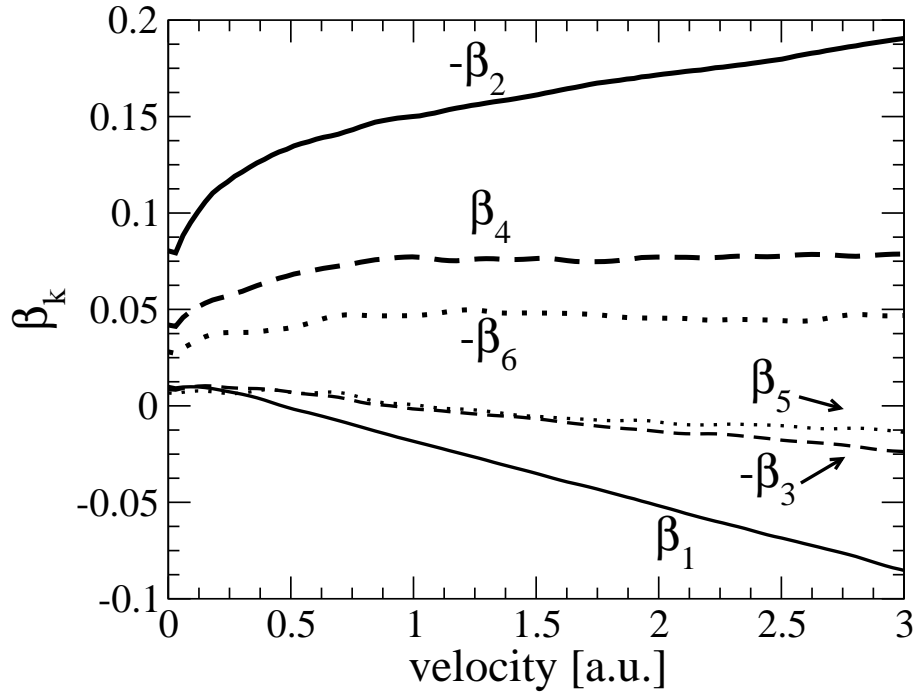


Fig. 3. Multipole expansion parameter of the CEP  $\beta_k(v)$  for a foil thickness of  $d = 25 \mu\text{g}/\text{cm}^2$  as a function of the electron velocity in the rest frame of the projectile ion. Sign of  $\beta_k$  changed as indicated in order to separate even and odd multipoles.

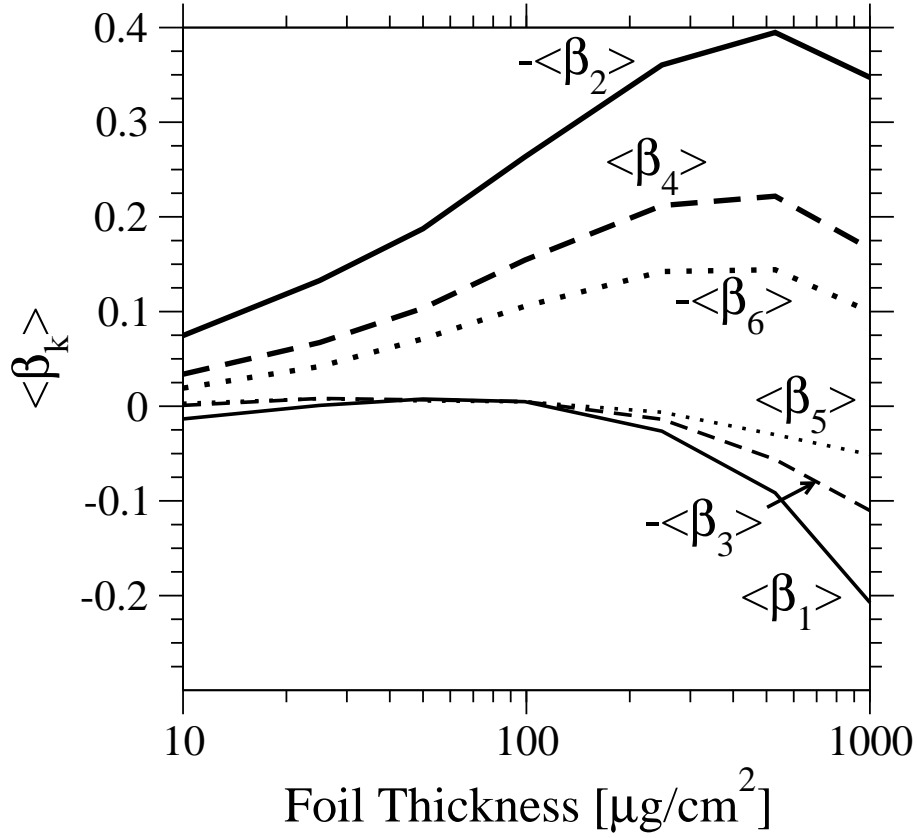


Fig. 4. Average of  $\beta_k(v)$  for the CEP within  $v \leq 1 a.u.$  as a function of the target thickness. Sign of  $\langle \beta_k \rangle$  changed as indicated in order to separate even and odd multipoles.

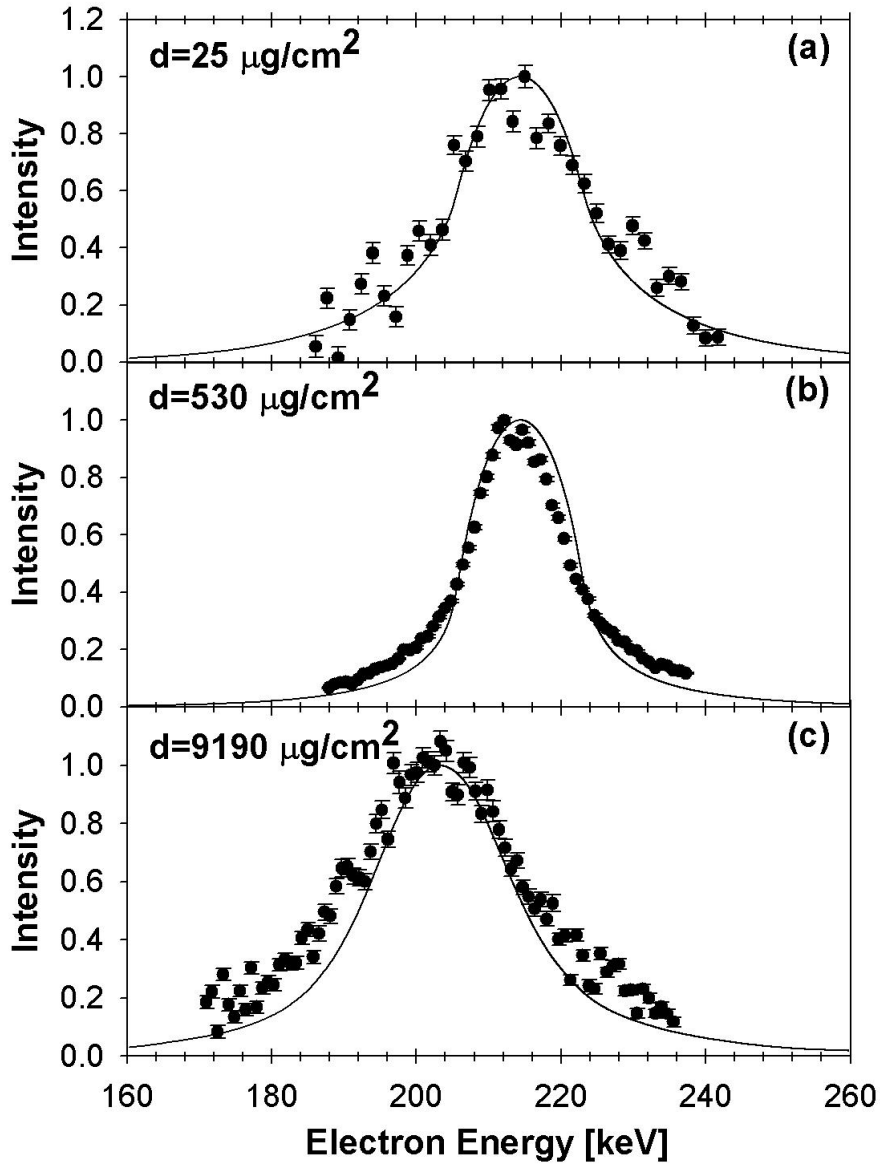


Fig. 5. Comparison of the recent theoretical calculation (solid line) with experimental data (symbols) for convoy electrons emitted by the transport of an  $\text{Ar}^{17+}$  ion (390 MeV/amu) through a carbon foil of following thickness: (a)  $25 \mu\text{g}/\text{cm}^2$  (2500 a.u.); (b)  $530 \mu\text{g}/\text{cm}^2$ ; (c)  $9190 \mu\text{g}/\text{cm}^2$ . Theoretical data have been convoluted with the experimental resolution ( $\Delta\theta = \pm 1^\circ$ ,  $\Delta E = \pm 9\text{keV}$ ).